Interaction of Proteins in Solution from Small-Angle Scattering: A Perturbative Approach

Francesco Spinozzi,* Domenico Gazzillo,[†] Achille Giacometti,[†] Paolo Mariani,* and Flavio Carsughi[‡]

*Istituto di Scienze Fisiche, Università di Ancona, and INFM Unità di Ancona, I-60131 Ancona, Italy; [†]Dipartimento di Chimica Fisica, Università di Venezia, and INFM Unità di Venezia, I-30123 Venezia, Italy; [‡]Facoltà di Agraria, Università di Ancona, and INFM Unità di Ancona, I-60131 Ancona, Italy

ABSTRACT   In this work an improved methodology for studying interactions of proteins in solution by small-angle scattering is presented. Unlike the most common approach, where the protein-protein correlation functions $g_{ij}(r)$ are approximated by their zero-density limit (i.e., the Boltzmann factor), we propose a more accurate representation of $g_{ij}(r)$ that takes into account terms up to the first order in the density expansion of the mean-force potential. This improvement is expected to be particulary effective in the case of strong protein-protein interactions at intermediate concentrations. The method is applied to analyze small-angle x-ray scattering data obtained as a function of the ionic strength (from 7 to 507 mM) from acidic solutions of β-lactoglobulin at the fixed concentration of 10 gl^{-1}. The results are compared with those obtained using the zero-density approximation and show significant improvement, particularly in the more demanding case of low ionic strength.

INTRODUCTION

The study of protein-protein interactions in solution and the determination of both the physical origin of long-range interactions and the geometry and energetics of molecular recognition can provide the most effective way of correlating structure and biological functions of proteins. In recent years a large effort has been devoted to improve the understanding of interactions between macromolecules in solution. In particular, it has been widely recognized that the evaluation of electrostatic potentials can produce quantitative predictions and that factors such as self-energy, polarizability, and local polarity can be biologically crucial (Halgren and Damm, 2001; Sheinerman et al., 2000). Nevertheless, major conceptual and practical problems still exist, and concern, for instance, the experimental techniques required to measure interaction potentials under physiologically relevant conditions and a clarification of the role of the solvent and of the protein shape and charge anisotropy.

Several biophysical methods can be used for extracting quantitative data on protein-protein interactions, even if a detailed analysis of the long-range interactions has to date been limited to few associating colloids (Chen and Lin, 1987; Itri and Amaral, 1991) and has usually been based on light scattering or osmotic stress methods (Parsegian and Evans, 1996). However, small-angle scattering (SAS) is certainly the most appropriate tool for studying the whole structure of protein solutions, because of the small perturbing effects on the system and the possibility of deriving information on the structural properties and interactions under very different experimental conditions (pH, ionic strength, temperature, presence of cosolvents, ligands, denaturing agents, etc.).

In most analyses of SAS data particle interactions are disregarded, assuming either large separation or weak interaction forces. The interactions among macromolecules determine their spatial arrangement, which can be described by correlation functions. These functions may be related, for instance via integral equations, to the direct pair potentials, describing the interaction between two particles. When the average distance among particles is large or the interaction potentials are weak, the influence of the average structure factor of the system (i.e., the Fourier transform of the average correlation function) may be negligible inside the considered experimental angular window, and the particles can be reckoned as completely uncorrelated. Under these conditions, the SAS intensity appears to depend only upon the average form factor. Note that this approximation of neglecting all intermolecular forces is used in most applications of x-ray or neutron SAS (Kozin et al., 1997; Chacón et al., 1998).

When the above conditions are not verified, then particles cannot be considered uncorrelated, and the average structure factor cannot be neglected in the expression of the SAS intensity. In this case data analysis is far more complicated. In principle, asymptotic behaviors could be used to separate the SAS intensity into (average) form and structure factors (Abis et al., 1990). If the particle form factors are known, an experimental average structure factor can be extracted by dividing the intensity by the average form factor. Then, some insight into the intermolecular forces may be obtained by comparison with the theoretical structure factor calculated from some interaction model, by using analytical or numerical methods from the statistical mechanical theory of liquids (Hansen and McDonald, 1986).

Unfortunately, the most powerful and accurate techniques provided by this theory—such as Monte Carlo and molecular dynamics computer simulations and integral

equations—can hardly be included into a typical best-fit procedure for analyzing experimental data. Working at very low concentrations, a first possibility of improving over the crude recipe of neglecting the average structure factor is to evaluate that quantity by approximating the pair correlation functions $g_{ij}(r)$ with their zero-density limit, given by the Boltzmann factor (Velev et al., 1997). In the present paper we shall show that this zero-density approximation becomes quite unusable at the usual protein concentrations when the ionic strength is low, i.e., in the presence of strong electrostatic interactions. Clearly, it would be desirable to find an alternative, simple but reasonably accurate, way for computing the average structure factor of globular proteins at low or moderate concentrations. This is the major aim of our paper.

Although the new proposal is methodological and thus applicable, in principle, to a wide class of spherically symmetric interaction models, it will be illustrated on a concrete case, as a part of a more general study on structural properties of a particular protein in solution, β-lactoglobulin (βLG).

In a previous paper (Baldini et al., 1999), which provides a natural introduction to the present work, all long-range protein-protein interactions were neglected and the average structure factor was assumed to be unity. That investigation reported experimental data concerning structural properties of βLG in acidic solutions (pH 2.3), at several values of ionic strength in the range 7-507 mM (Baldini et al., 1999). Photon correlation spectroscopy and small-angle x-ray scattering (SAXS) experiments gave a clear evidence of a monomer-dimer equilibrium affected by the ionic strength. In the angular region where SAXS experiments were performed the contribution of long-range protein-protein interactions was expected to be rather small. Accordingly, SAXS data were analyzed only in terms of βLG monomer and dimer form factors, which were calculated very accurately. Short-range forces responsible for protein aggregation were taken into account only implicitly through a chemical association equilibrium, used to evaluate the dimerization fraction. A global fit procedure allowed the determination of the monomer effective charge and protein dissociation free energy within a wide range of ionic strength (Baldini et al., 1999).

In the present paper we shall investigate, within the same physical system, the long-range protein-protein interactions, which can strongly influence the small-angle scattering at low ionic strength. To this aim, two issues have to be addressed. First, one needs to extend the experimental SAXS angular region to lower values of the scattering vector, where long-range forces play an important role. Second, one has to select an accurate and tractable theoretical scheme for calculating the average structure factor to be used in the fit of experimental data. Both tasks have been accomplished in this work.

We first report a new set of SAXS measurements on βLG performed under the same experimental conditions as Baldini and co-workers (Baldini et al., 1999), but for smaller angles. These data unambiguously display a lowering in the scattering intensity at small angles, with a progressive development of an interference peak, when ionic strength is low. This occurrence is a clear signal of strong protein-protein interactions, and we shall show that it can be simply interpreted in terms of screened electrostatic repulsions among charged macroions.

Next, we shall propose an improvement for the calculation of the theoretical average structure factor, based upon a new approximation to the protein-protein correlation functions $g_{ij}(r)$. Starting from the density expansion of the corresponding mean-force potentials, we shall show that the simple addition of the first-order perturbative correction to the direct pair potentials leads to a marked progress with respect to the use of the Boltzmann factor, while retaining the same level of simplicity. The new approximation is indeed able to predict, at low ionic strength, the interference peak observed in the experimental scattering intensity, and consequently it leads to a significantly improved fit.

We stress, in advance, that a check of the unavoidable limits of validity of the proposed approach will not be treated here. A further study involving a comparison with more accurate theoretical results (from Monte Carlo or molecular dynamics, and from integral equations) is, of course, desirable, but goes beyond the scope of the present paper, and will be left for future work.

BASIC THEORY

Because of the presence of an aggregation equilibrium, a βLG solution contains two different forms of macroions (protein monomers and dimers) embedded in a suspending fluid and in a sea of microions, which include both counterions neutralizing all protein charges and small ions originated from the addition of electrolyte salts. To represent such a system, we shall use a simple "two-component macroion model," which effectively takes into account only protein particles. Within this scheme, which is usually referred to as the Derjaguin-Landau-Vervey-Overbeek (DLVO) model (Vervey and Overbeek, 1948), the suspending fluid (solvent) is represented as a uniform dielectric continuum and all microions are treated as point-like particles. The presence of both solvent and microions appears only in the macroion-macroion *effective* potentials. A further simplification follows from the assumption of spherically symmetric interactions. We note that in our model, components 1 and 2 correspond to monomers and dimers, respectively. Before addressing the specific system under investigation, it is convenient to recall some basic points of the general theory.

Scattering functions

The macroscopic differential coherent scattering cross-section $d\Sigma/d\Omega$, obtained from a SAS experiment, is related to the presence of scattering centers, i.e., density and/or structural inhomogeneities, and can yield quantitative information about their dimensions, concentration, shape and interaction potentials. The cross-section is proportional to the "contrast," namely the difference of electron density multiplied by the classical electron radius (or scattering length density in the neutron case) between the scattering centers and the surrounding medium; in the case of biological samples, this quantity can also be tuned to obtain more detailed information about the scattering structures (contrast variation technique (Jacrot, 1976)). Proteins in solution represent an excellent example of inhomogeneities for SAS measurements, due to their high contrast with x-rays (and with neutrons). The general equation for the SAS intensity is

$$\frac{d\Sigma}{d\Omega}(\mathbf{Q}) = \frac{1}{V}\left\langle\left|\int_V d\mathbf{r}\delta\rho(\mathbf{r})e^{i\mathbf{Q}\cdot\mathbf{r}}\right|^2\right\rangle, \quad (1)$$

with $\mathbf{Q}$ being the exchanged wave vector, with magnitude $Q = (4\pi/\lambda)\sin\theta$, where λ represents the incident radiation wavelength and 2θ is the full scattering angle. The integral in Eq. 1 is extended over the sample volume V, with $\mathbf{r}$ being the position vector and $\delta\rho(\mathbf{r})$ the fluctuation with respect to a uniform value, ρ_0, of the local electron density multiplied by the classical electron radius (or simply the scattering length density in the case of neutrons). Angle brackets represent an ensemble average over all possible configurations of the proteins in the sample.

Equation 1 can be reduced to a simpler form when the interactions are spherically symmetric. Using a "two-phase" representation of the fluid (only one type of homogeneous scattering material with scattering density ρ_P inside proteins, embedded in a homogeneous solvent phase with density ρ_0) yields

$$\frac{d\Sigma}{d\Omega}(Q) = (\Delta\rho)^2\left\{\sum_{i=1}^p n_i V_i^2[\langle F_i^2(\mathbf{Q})\rangle_{\omega_Q} - \langle F_i(\mathbf{Q})\rangle_{\omega_Q}^2]\right.$$
$$\left. + \sum_{i,j=1}^p (n_i n_j)^{1/2}V_i V_j\langle F_i(\mathbf{Q})\rangle_{\omega_Q}\langle F_j(\mathbf{Q})\rangle_{\omega_Q}S_{ij}(Q)\right\} \quad (2)$$

where $\Delta\rho \equiv \rho_P - \rho_0$ represents the contrast, p the number of protein species (2 for our solutions with monomers and dimers), n_i the number density of species i, V_i its volume, $F_i(\mathbf{Q})$ its form factor, $S_{ij}(Q)$ the Ashcroft-Langreth partial structure factor, and $\langle...\rangle_{\omega_Q}$ denotes an orientational average.

The partial structure factors (Ashcroft and Langreth, 1967) are defined as

$$S_{ij}(Q) = \delta_{ij} + 4\pi(n_i n_j)^{1/2}\int_0^\infty dr r^2[g_{ij}(r) - 1]\frac{\sin(Qr)}{Qr}, \quad (3)$$

in terms of the three-dimensional Fourier transform of $g_{ij}(r) - 1$, where $g_{ij}(r)$ is the pair correlation function (or radial distribution function, RDF) between particles of species i and j, and δ_{ij} is the Kronecker's delta.

Finally, the average form and structure factors, $P(Q)$ and $S_M(Q)$, are

$$P(Q) = (\Delta\rho)^2\sum_{i=1}^p n_i V_i^2\langle F_i^2(\mathbf{Q})\rangle_{\omega_Q}, \quad (4)$$

$$S_M(Q) = \frac{d\Sigma}{d\Omega}(Q)/P(Q). \quad (5)$$

Protein form factors

The angular averaged form factor of species i can be written as

$$\langle F_i(\mathbf{Q})\rangle_{\omega_Q} = \int_0^\infty dr p_i^{(1)}(r)\frac{\sin(Qr)}{Qr}, \quad (6)$$

where $p_i^{(1)}(r)$ represents the probability for the ith species that a point at distance r from the protein center of mass lies inside the macromolecule. Similarly, the angular averaged squared form factor is given by Guinier and Fournet (1955)

$$\langle F_i^2(\mathbf{Q})\rangle_{\omega_Q} = \int_0^\infty dr p_i^{(2)}(r)\frac{\sin(Qr)}{Qr} \quad (7)$$

where $p_i^{(2)}(r)$ represents the probability for the ith species to find a segment of length r with both ends inside the macromolecule. Both integrals of $p_i^{(1)}(r)$ and $p_i^{(2)}(r)$ are normalized to unity. These distribution functions have been calculated from the crystallographic structures of both the monomer and dimer forms of the protein, as described in Baldini et al. (1999), Mariani et al. (2000), briefly recalled in Appendix A, and discussed in Materials and Methods.

Protein-protein interaction potentials

The choice of the proper potential is a rather delicate matter and depends on the investigated system. For instance, in a study on lysozyme (Kuehner et al., 1997) the protein-protein interaction was assumed to be the sum of four contributions, namely a hard-sphere term, an electrostatic repulsion, an attractive dispersion potential, and a short-range

attraction. In a different study, on lysozyme and chymotrypsinogen (Velev et al., 1997), five contributions were considered: charge-charge repulsion, charge-dipole, dipole-dipole and van der Waals attractions, and further complex short-range interactions. In this paper we follow a different route motivated by the fact that the presence of several interaction terms may obscure the relative importance of each of them. Moreover, the choice of a very refined potential would be in striking contrast with the very crude approximations used in calculating the RDFs. On this basis we shall search for the simplest possible model potential that is still capable of capturing the essential features of the system. It will be the sum of two repulsive contributions:

$$u_{ij}(r) = u_{ij}^{HS}(r) + u_{ij}^{C}(r) \qquad (8)$$

where

$$u_{ij}^{HS}(r) = \begin{cases} +\infty & 0 \le r < R_i + R_j \\ 0 & r \ge R_i + R_j \end{cases} \qquad (9)$$

is a hard-sphere (HS) term which accounts for the excluded-volume effects (R_i being the radius of species i) and

$$u_{ij}^{C}(r) = \frac{Z_i Z_j e^2}{\epsilon(1 + \kappa_D R_i)(1 + \kappa_D R_j)} \frac{\exp[-\kappa_D(r - R_i - R_j)]}{r} \qquad (10)$$

represents a screened Coulomb repulsion between the macroion charges, which are of the same sign. This term has the same Yukawa form as in the Debye-Hückel theory of electrolytes, but the coupling coefficients are of DLVO type (Vervey and Overbeek, 1948). Here, e is the elementary charge, ϵ the dielectric constant of the solvent, and the effective valency of species i, Z_i, may depend on the pH. The inverse Debye screening length κ_D, defined as

$$\kappa_D = \left[\frac{8\pi\beta e^2 N_A}{\epsilon}(I_S + I_c) \right]^{1/2}, \qquad (11)$$

depends on temperature ($\beta = (k_B T)^{-1}$) and on the ionic strength of all microions. I_S and I_c represent the ionic strength of all added salts (S) and of the counterions (c), respectively. Both these terms are of the form $(1/2)\sum_i c_i^{micro}(Z_i^{micro})^2$, with $c_i^{micro} = n_i^{micro}/N_A$ being the molar concentration of microspecies i (N_A is Avogadro's number). I_c is related to the macroion number densities n_1 and n_2 ($1 =$ monomer, $2 =$ dimer) through the electroneutrality condition, according to which the counterions must neutralize all macroion charges, i.e., $n_c|Z_c| = n_1|Z_1| + n_2|Z_2|$. Notice that the dependence of κ_D on I_S implies that the strength of the effective potential $u_{ij}^{C}(r)$ can largely be varied by adding an electrolyte to the solution.

We have explicitly checked that the addition of an attractive term with the form of a Hamaker potential $u_{ij}^{H}(r)$ (Israelachvili, 1992) does not alter our final conclusions. The basic reason for this can be traced back to the fact that van der Waals attractions may be completely masked by $u_{ij}^{C}(r)$ when the electrostatic repulsion is strong, and are also negligible for moderately charged particles with a diameter smaller than 50 nm (Nägele, 1996). Moreover, $u_{ij}^{H}(r)$ diverges at $r = R_i + R_j$, so that its applicability could be preserved only by the addition of a non-interpenetrating hydration/Stern layer (Baldini et al., 1999; Kuehner et al., 1997).

We stress the fact that some attractive interactions must, however, be present in the system, because they are responsible for the aggregation of monomers into dimers and determine the value of the monomer molar fraction x_1, which is required to complete the definition of our model. However, due to the complexity of these interactions (including hydrogen bonding), a clear understanding of their explicit functional forms is still lacking. Therefore, following Baldini et al. (1999), we will account for them indirectly, by using a chemical association equilibrium to fix x_1. The dissociation free energy, which determines the equilibrium constant, is written as a sum of two contributions, i.e.

$$\Delta G_{dis} = \Delta G_{el} + \Delta G_{nel}, \qquad (12)$$

where ΔG_{el} is an electrostatic term calculated within the Debye-Hückel theory, and ΔG_{nel} is an unknown non-electrostatic contribution, which will be left as a free parameter in the best-fit analysis.

Radial distribution functions

Given a model potential, one has to calculate the corresponding RDF $g_{ij}(r)$, which can be expressed by the *exact* relation

$$g_{ij}(r) = \exp[-\beta W_{ij}(r)], \qquad (13)$$

$$-\beta W_{ij}(r) = -\beta u_{ij}(r) + \omega_{ij}(r) \qquad (14)$$

where $W_{ij}(r)$ is the potential of mean force, which includes the direct pair potential $u_{ij}(r)$ and $-\beta^{-1}\omega_{ij}(r)$, i.e., the indirect interaction between i and j due to their interaction with all remaining macroparticles of the fluid. In the zero-density limit, $\omega_{ij}(r)$ vanishes and $g_{ij}(r)$ reduces to the Boltzmann factor, i.e.

$$g_{ij}(r) = \exp[-\beta u_{ij}(r)] \quad \text{as } n \to 0, \qquad (15)$$

which represents a zeroth-order approximation, frequently used in the analysis of experimental scattering data ($n \equiv \sum_m n_m$ is the total macroparticle number density).

The most common procedure for determining an accurate $g_{ij}(r)$ or, equivalently, the correction term $\omega_{ij}(r)$, would be to solve the Ornstein-Zernike (OZ) integral equations of the liquid state theory, within some approximate closure relation (Hansen and McDonald, 1986). This can typically be done numerically, with the exception of few simple cases

(for some potentials and peculiar closures) where the solution can be worked out analytically.

For our hard-sphere Yukawa potential (neglecting the Hamaker term), the OZ equations do admit analytical solution when coupled with the "mean spherical approximation" (MSA) (Blum and Hoye, 1978; Ginoza, 1990; Hayter and Penfold, 1981). Nevertheless, at low density and for strong repulsion the MSA RDFs may assume unphysical negative values close to interparticle contact (Nägele, 1996). To overcome this difficulty, it would be possible to utilize an analytical "rescaled MSA" (Nägele, 1996; Hansen and Hayter, 1982; Ruiz-Estrada et al., 1990) or to resort to different closures (Rogers-Young approximation or "hypernetted chain" closure), which compel numerical solution (Rogers and Young, 1984; Zerah and Hansen, 1986; Wagner et al., 1991; Krause et al., 1991; D'Aguanno and Klein, 1992; D'Aguanno et al., 1992; Nägele et al., 1993).

More generally, when only numerical solutions are feasible, integral equation algorithms can hardly be included in a best-fit program for the analysis of SAS results. The use of analytical solutions, or simple approximations requiring only a minor computational effort, is clearly much more advantageous when fitting experimental data. The zeroth-order approximation given in Eq. 15 avoids the problem of solving the OZ equations, but is largely inaccurate except, perhaps, at very low densities.

To improve over this zeroth-order approximation to the RDFs, the basic idea put forward in the present work hinges upon the expansion of the potential of mean force into a power series of the total number density n (Meeron, 1958). Neglecting all terms beyond the first-order one, Eq. 13 then becomes

$$g_{ij}(r) = \exp[-\beta u_{ij}(r) + \omega_{ij}^{(1)}(r)n]. \qquad (16)$$

By construction, this expression is never negative, thus avoiding the major drawback of MSA. The explicit expression for the perturbative correction $\omega_{ij}^{(1)}(r)$ is given in Appendix B. The considered first-order approximation substantially improves the accuracy of the RDFs with respect to Eq. 15, while remaining at nearly the same level of simplicity (see Appendix B). Moreover, it is to be stressed that the usage of the new approximation is not restricted to the model of this paper, but the proposed calculation scheme can be equally well applied to different spherically symmetric potentials.

MATERIALS AND METHODS

Samples

A bovine milk βLG B stock solution (concentration 40 gl^{-1} was obtained by ionic exchange of protein samples against a 12 mM phosphate buffer (ionic strength $I_S = 7$ mM and pH = 2.3) (Baldini et al., 1999). Nine samples at ionic strength 7, 17, 27, 47, 67, 87, 107, 207, and 507 mM were then prepared by adding appropriate amounts of NaCl. The final protein concentrations were $\sim$10 gl^{-1}.

The monomeric βLG is composed of 162 amino acid residues and has a molecular weight of 18,400. The excluded protein volume has been calculated from the amino acid volumes, as reported by Jacrot and Zaccai (Jacrot, 1976; Jacrot and Zaccai, 1981). The monomer volume results to be $V_1 = 23,400$ Å^3; hence, the βLG electron density is $\rho_P = 0.418$ eÅ^{-3}. By considering the basicity of the amino acids, at pH 2.3 the monomer charge would be near 20e. This result is confirmed by the Gasteiger-Marsili method (Gasteiger and Marsili, 1980), assuming that all amino groups NH$_2$ are protonated at pH 2.3. The crystallographic structure of βLG both in monomer and in dimer form can be found in the Protein Data Bank, entry 1QG5 (Oliveira et al., 2001). A sketch of βLG dimer structure can be found in Fig. 1 of Baldini et al. (1999). It can be observed that all 20 basic amino acids are on the protein surface, but two of them are at the monomer-monomer interface; therefore at pH 2.3 the ratio Z_2/Z_1 between dimer and monomer charges could be $\sim$1.8.

SAXS experiments

SAXS measurements were collected at the Physik Department of the Technische Universität München (Germany) using a rotating-anode generator. The radiation wavelength was $\lambda = 0.71$ Å and the temperature 20°C. The Q range was 0.035–0.1 Å^{-1}. βLG samples were measured in quartz capillaries with a diameter of 2 mm and a thickness of 10 μm (Hilgenberg, Malsfeld, Germany). X-ray patterns were collected by a two-dimensional detector and radially averaged. The scattering from a solvent capillary was subtracted from the data after correction for transmission, capillary thickness, and detector efficiency.

Best-fit analysis

A previous analysis of SAXS data for similar samples in the range $Q = 0.07$–0.3 Å^{-1} has been recently reported by some of us (Baldini et al., 1999). In the present work we have extended these experiments to the range $Q = 0.035$–0.1 Å^{-1}, where protein-protein interactions are expected to play a major role. The two sets have then been combined into a single set of measurements with Q ranging from 0.035 to 0.3 Å^{-1}.

As regards the calculation of the monomer and dimer form factors, it is well known that the scattering form factor of a biomolecule in solution depends on the crystallographic coordinates and the form factors of all constituent atoms, as well as on the hydration shell of the resulting macroparticle. Computer programs such as CRYSOL (Svergun et al., 1995) are able to calculate such a form factor, taking all the above-mentioned variables into account. It is also widely accepted that the SAS technique is a low-resolution one, and approximating the βLG protein by a homogeneous scattering particle yields comparable results up to $Q = 0.4$ Å^{-1}, as we have tested by checking our method against the results of the CRYSOL software. The equivalent homogeneous scattering particle has a shape defined by the envelope of the van der Waals spheres centered on each atom. The SAS community often exploits the Monte Carlo method to calculate the form factor of a given shape (Henderson, 1996). We have modeled the hydration shell with a semi-Gaussian function instead of the linear one proposed by Svergun et al. (1997). Our simple and efficient method has already been applied with success in previous works (Baldini et al., 1999; Mariani et al., 2000).

The Monte Carlo method used to calculate the distribution functions $p_i^{(1)}(r)$ and $p_i^{(2)}(r)$ of both monomers ($i = 1$) and dimers ($i = 2$) from their crystallographic structures is outlined in Appendix A. Then the form factors $\langle F_i(\mathbf{Q})\rangle_{\omega_Q}$ and $\langle F_i^2(\mathbf{Q})\rangle_{\omega_Q}$ have been obtained through Eqs. 6 and 7, by calculating the radial integrals with a grid size of 1 Å up to a maximum r corresponding to $P_i^{(1)}(r) = 0$ and $P_i^2(r) = 0$ ($i = 1, 2$).

According to the dissociation free energy model described in Baldini et al. (1999), the monomer molar fraction x_1 is a function of the ionic strength I_S. This suggests the possibility of a simultaneous fit for all SAXS intensity curves using just few parameters, all independent on I_S. In particular, as in

Baldini et al. (1999), the following parameters have been fixed: the dielectric constant of the solvent, $\epsilon = 78.5$; the experimental temperature, $T = 293$ K; the ratio between the effective charges of dimer and monomer, $Z_2/Z_1 = 1.8$; the monomer and dimer "bare" radii, $R_1 = 19.15$ Å and $R_2 = 2^{1/3}R_1$. The choice for R_2 is easily understood if we recall that our model of long-range interactions involves the approximation of considering a dimer as a sphere with a volume twice as large as the monomer. This introduction of an equivalent sphere is a simplifying approximation often used by the SAS community. However, we have calculated the form factor of the dimer from its exact, rather elongated form.

In the global fit the only free parameters are therefore Z_1 and ΔG_{nel}, the non-electrostatic free energy. The merit functional to be minimized was defined as

$$\chi^2 = \frac{1}{N_S} \sum_{m=1}^{N_S} \bar{\chi}_m^2$$

$$\bar{\chi}_m^2 = \frac{1}{N_{Q,m}} \sum_{i=1}^{N_{Q,m}} \left\{ \frac{[d\Sigma/d\Omega]_m^{exp}(Q_i) - \kappa_m[d\Sigma/d\Omega]_m^{fit}(Q_i) - B_m}{\sigma_m(Q_i)} \right\}^2$$

(17)

where N_S is the number of scattering curves under analysis, $N_{Q,m}$ is the number of experimental points in the mth curve, and $\sigma_m(Q_i)$ is the experimental uncertainty on the intensity value at Q_i. $[d\Sigma/d\Omega]_m^{fit}(Q_i)$ is the corresponding cross-section predicted by the model by using Eq. 2; for each experiment, the calibration factor κ_m and the flat background B_m have been adjusted from a linear least-squares fit of $[d\Sigma/d\Omega]_m^{exp}(Q)$. The partial structure factors, Eq. 3, have been calculated with an integration upper limit of $r = 500$ Å and a grid size of 1 Å.

The physical meaning of the "flat background" requires a comment because constant subtraction is usually accepted for neutron scattering, but not for x-ray scattering. Introducing these backgrounds is suggested by observing that one of the major experimental problems with x-rays is the exact determination of the transmission factor. A non-exact value would result into a nonperfect subtraction of the background due to the electronic noise. However, as shown in Table 2, the low values obtained for B_m, as compared to the values of the scaling factors, indicate that these parameters play a minor role in the data analysis.

Typical calculation times for the best-fit on a Digital Alpha 433 are a few minutes for the zeroth-order approximation and ~20 h for the first-order one. The effect of experimental errors on the fitting parameters has been determined using a sampling method. For each scattering curve we start from $N_{Q,m}$ intensities $[d\Sigma/d\Omega]_m^{exp}(Q_i)$ with their experimental standard deviation, and we generate N_I new data sets (for βLG we used $N_I = 15$) by sampling from $N_{Q,m}$ Gaussians of width $\sigma_m(Q_i)$ centered at the observed values. Each data set generated for all curves is then analyzed with the global fit algorithm described earlier. The errors on the fitting parameters, Z_1 and ΔG_{nel}, and on the scaling parameters, κ_m and B_m, are obtained by calculating their values from each data set and, finally, their standard deviation from the first value.

RESULTS AND DISCUSSION

Fig. 1 depicts the experimental results for the x-ray intensity $[d\Sigma/d\Omega](Q)$ as a function of the transferred momentum Q at several values of ionic strength. Here, instead of the usual logarithmic scale, we have preferred the use of a linear scale, to let the reader appreciate more easily the small differences between experimental data and theoretical curves. On a log scale these differences would be hardly visible.
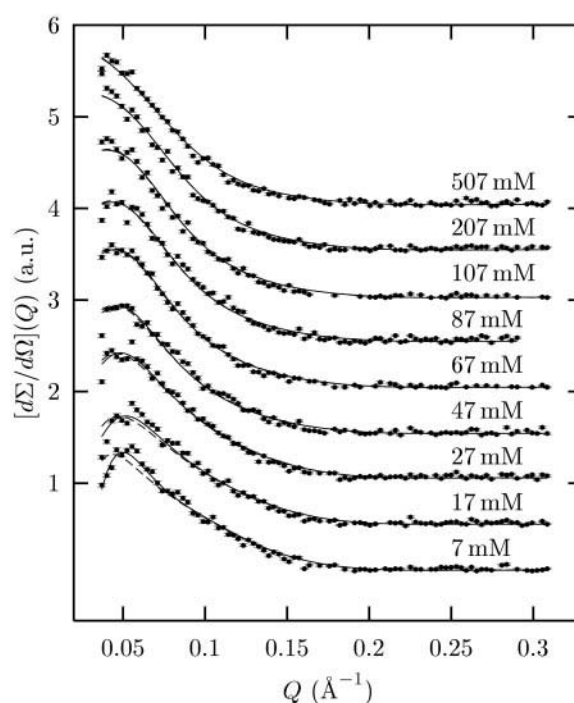
FIGURE 1 SAXS linear profiles for the βLG at pH 2.3 and concentration 10 gl^{-1} in different ionic strength conditions (as indicated above each curve). Points are experimental results, whereas the dashed and the solid lines represent the best fits obtained by applying the zeroth- and first-order approximations of the pair correlation functions, respectively. The curves are scaled for clarity by a factor of 0.5.

Our measurements clearly show the formation and evolution of an interference peak at small angles as the ionic strength decreases. The appearance of such a peak is evidently due to increasing protein-protein interactions. In the same figure, the performance of our first-order approximation is compared with that of the commonly used zeroth-order one. The first-order approximation yields a fit of rather good quality through the whole measured Q-range. The development of the interference peak, underestimated by the zeroth-order approximation, is now well reproduced, indicating that the main physical features of the βLG solution are indeed taken into account by our simple interaction model.

In Fig. 2 the theoretical results for the average structure factor $S_M(Q)$ are shown along with the experimental data. While at high I_S (i.e., at weak effective interactions) the two approximations are practically undistinguishable, for $I_S \leq 27$ mM the first-order results outplay the zeroth-order ones, mainly in the low-Q region.

A more transparent comparison between the two approximations is carried out in Fig. 3 at the level of RDFs. As I_S decreases, the first-order $g_{ij}(r)$ become strongly different from the zeroth-order ones, exhibiting a peak of increasing height. In terms of potentials of mean force, $g_{ij}(r) > 1$ in some regions (mainly for $I_S \leq 27$ mM) implies that
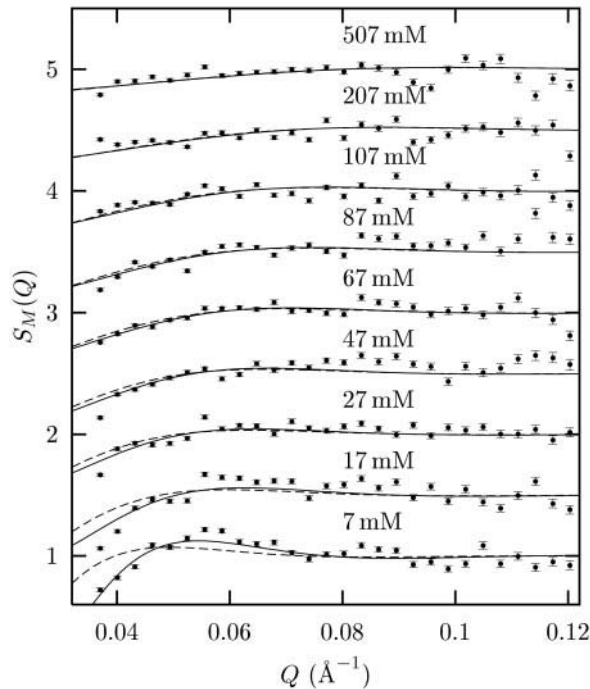
FIGURE 2 Measured structure factors $S_M(Q)$ for the βLG at pH 2.3 and concentration 10 gl^{-1} in different ionic strength conditions (as indicated above each curve). The best-fit lines resulting from the simultaneous analysis of the corresponding SAXS curves (Fig. 1) using the zeroth-order (*dashed line*) and first-order (*solid line*) approximations of the pair correlation functions are reported. Data for $Q > 0.12$ Å^{-1} are not shown for clarity.
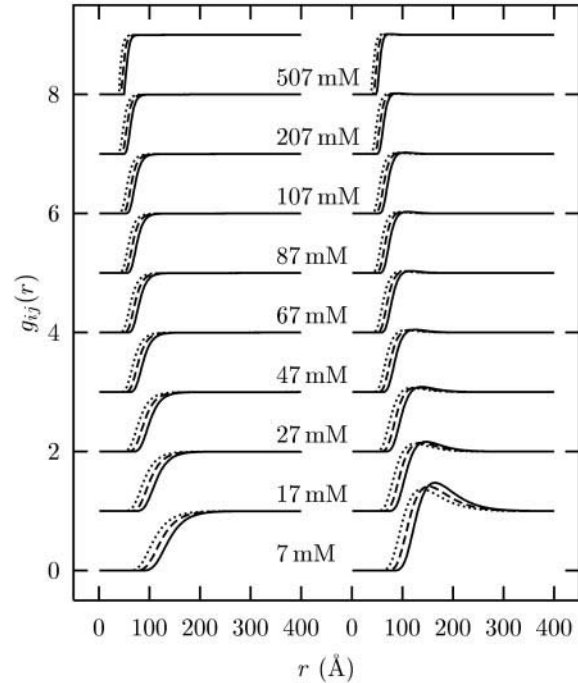

FIGURE 3 Partial correlation functions $g_{ij}(r)$ resulting from the simultaneous analysis of the nine SAXS curves of Fig. 1 (the ionic strength, I_S, is indicated near each set of curves) by applying the zeroth-order (*left column*) and first-order (*right column*) approximations in the density expansion of the mean-force potential. Depicted are the monomer-monomer, $g_{11}(r)$ (*dotted lines*), the monomer-dimer, $g_{12}(r)$ (*dashed lines*), and the dimer-dimer, $g_{22}(r)$ (*solid line*), correlation functions.

$W_{ij}(r) < 0$, although $u_{ij}(r)$ always remains positive. The first-order correction $\omega_{ij}^{(1)}(r)n$ (Eq. B1) therefore corresponds to an *attractive* contribution, due to an "osmotic depletion" effect (Asakura and Oosawa, 1954) exerted on two given macroparticles by the remaining ones. This many-body effect is clearly lacking in the zeroth-order approximation, as depicted in Fig. 3. Depletion forces arise when two protein molecules are close together. In this case the pressure exerted on these molecules by all other macroparticles becomes anisotropic, leading to a strong indirect protein-protein attraction, even though all direct interactions are repulsive.

It is worth stressing that the behavior of the first-order $g_{ij}(r)$ at low ionic strength could be reproduced even by the zeroth-order approximation, but only at the cost of adding some unnecessary, and somewhat misleading, density-dependent attractive term to the direct pair potentials. Our model, based only on the physically sound repulsive part of the DLVO potential, turns out to be rather accurate for the purposes of the present paper. As previously discussed, we have also performed some calculations including a Hamaker term into our perturbative scheme, without finding any significative change in the first-order results with respect to the previous ones.

The first-order RDFs shown in Fig. 3 are undoubtedly correctly shaped, although the peak heights might be modified by the neglected second- and higher-order corrections to the potentials of mean force. Unfortunately, an estimate for the magnitude of the successive perturbative terms (depending on both concentration and charge of the protein molecules) is a far more complicated task and goes beyond the scope of the present paper. Since the resulting protein charges (see Table 1) are relatively large, it is reasonable to expect that the contribution of the higher-order terms might be appreciable. As the protein concentration increases, this correction becomes more and more significant, and eventually the rather good performance of our first-order approximation could break down.

TABLE 1 Comparison of the fitting parameters (the monomer effective charge, Z_1, and the nonelectrostatic free energy, ΔG_{nel}) and of the merit functional χ^2 resulting from the simultaneous analysis of the nine SAXS curves of Fig. 1 by applying the zeroth- and first-order approximations of the pair correlation functions

Approximation	Z_1	$\Delta G_{nel}/k_B T$	χ^2
Zeroth	19.6 ± 0.1	14.8 ± 0.1	10.9
First	20.0 ± 0.2	16.6 ± 0.1	8.9

TABLE 2 Comparison of the scaling factors, κ_m, the flat backgrounds, B_m, and the merit functionals, $\bar{\chi}_m^2$ (Eq. 17), resulting from the simultaneous analysis of the nine SAXS curves of Fig. 1 by applying the zeroth- and first-order approximations of the pair correlation functions. The last entry (Var (%)) provides the relative variation between the zeroth- and first-order approximations

I_S (mM)	κ_m (10^{-3} a.u. cm)		B_m (10^{-5} a.u.)		$\bar{\chi}_m^2$		
	Zeroth	First	Zeroth	First	Zeroth	First	Var (%)
7	1.450 ± 0.002	1.478 ± 0.002	4.62 ± 0.06	4.48 ± 0.06	14.2	8.0	-43.7
17	1.424 ± 0.002	1.424 ± 0.002	4.73 ± 0.05	4.73 ± 0.05	14.8	10.7	-27.7
27	1.619 ± 0.003	1.521 ± 0.003	4.79 ± 0.05	5.23 ± 0.05	10.9	8.7	-20.2
47	1.397 ± 0.003	1.293 ± 0.003	3.46 ± 0.05	3.98 ± 0.04	10.6	9.9	-6.6
67	1.443 ± 0.002	1.367 ± 0.002	3.78 ± 0.05	4.25 ± 0.06	7.7	5.5	-28.6
87	1.405 ± 0.003	1.351 ± 0.003	4.18 ± 0.06	4.47 ± 0.07	12.0	11.8	-1.7
107	1.493 ± 0.003	1.450 ± 0.002	2.06 ± 0.06	2.30 ± 0.06	9.3	8.2	-11.8
207	1.478 ± 0.002	1.457 ± 0.002	4.12 ± 0.06	4.23 ± 0.06	10.1	9.5	-5.9
507	1.529 ± 0.003	1.518 ± 0.003	3.68 ± 0.08	3.73 ± 0.08	8.3	8.0	-3.6

Because a direct computation of even the second-order corrections demands a high computational effort, the accuracy of the first-order approximation may alternatively be investigated by checking our RDF results against exact Monte Carlo or molecular dynamics simulation data relevant to the same model. A simpler indication about the limits of validity of our scheme may come from a systematic comparison with integral-equation predictions based upon more accurate closures. One could use, for instance, the multicomponent version of the "rescaled MSA" approach (Ruiz-Estrada et al., 1990), which has the advantage of being nearly fully analytical. However, if more accurate results are required, then the Rogers-Young closure (Rogers and Young, 1984) is preferable for our potential, but in this case the corresponding integral equations must be solved numerically. We have planned some investigations in this sense, and their results will be reported elsewhere. However, we believe that, at the considered protein concentration, the first-order approximation does yield the correct trend of the RDFs. It is our opinion that the inclusion of the neglected terms cannot alter the qualitative (or semiquantitative) picture of βLG interactions supported by our model, even if slightly different values for the best-fit parameters should be expected.

The parameter values resulting from the global best-fit procedure, using the zeroth-order and first-order approximations, are reported in Tables 1 and 2.

The improved quality of the fit corresponding to the first-order approximation can clearly be appreciated by comparing not only the global χ^2 value (Table 1), but above all the partial $\bar{\chi}_m^2$ ones (Table 2), in particular for $I_S \leq 27$ mM. Although the change of global χ^2 is not so large, all the values of $\bar{\chi}_m^2$ improve with the first-order approximation: the improvement is rather evident for the low ionic strength samples, while it becomes less and less important with increasing ionic strength. The proposed method is able to improve the goodness of the fit by $\sim$44% for the first sample (where the interference peak is more pronounced). The decrease of the relative variation, as the ionic strength

increases, is in agreement with the expected progressive weakening of protein-protein repulsions.

Note that the values of both fitting parameters, i.e., Z_1 and ΔG_{nel}, turn out to be very similar for both approximations. The scaling factors, κ_m, and the flat backgrounds, B_m, are also similar for all samples and for both approximations, confirming that no other effects, such as denaturation or larger aggregation, are really present.

CONCLUSIONS

In this paper we have presented a novel methodological approach to the study of protein-protein interactions using SAXS techniques. Our work builds upon a previous investigation by some of us (Baldini et al., 1999).

As widely discussed by Baldini et al., 1999, the structural properties of βLG in acidic solution, studied by light and x-ray scattering over a wide range of ionic strength and concentration, are consistent with the existence of monomers and dimers, and cannot be ascribed to a denaturation process.

Because the form factors of both the species are easily known, the so-called "measured" or average structure factor $S_M(Q)$ can be obtained from the ratio between experimental intensity and average form factor $P(Q)$ at a certain monomer fraction x_1. $S_M(Q)$ is related to the protein-protein effective interactions. Short-range attractive interactions like hydrogen bonds, responsible for the dimer formation and strongly depending on the monomer-monomer orientations, are taken into account using a quasi-chemical description of the thermodynamic equilibrium between monomer and dimer forms of βLG. Thus, in addition to the hardcore repulsions, the effective potentials of mean force only describe long-range monomer-monomer, monomer-dimer, and dimer-dimer electrostatic repulsions, which can be reduced to their orientational averages, depending only on the intermolecular distance r.

In the work by Baldini et al., 1999, all long-range protein-protein forces were neglected because the measured SAXS

intensity was spanning a Q-range where such interactions are essentially negligible. On the contrary, we have explicitly addressed this issue in the present work. To this aim, 1) we have extended the range of measured intensities to lower Q values to experimentally probe these long-range interactions, and 2) we have proposed a simple but efficient perturbative scheme, whose first terms are able to yield reasonably accurate RDFs for dilute or moderately concentrated solutions of globular proteins, with rather little computational effort. In particular, we have explicitly computed the zeroth- and first-order approximations and compared their results.

The improvement in the quality of the fit for $S_M(Q)$, obtained with the first-order correction for the potentials of mean force corresponding to the RDFs with respect to the standard zero-density approximation, is particularly visible at low ionic strength, where Coulomb repulsions are poorly screened. In this case, the new representation of the RDFs is able to reproduce the interference peak present in the experimental $S_M(Q)$, whereas the commonly used zero-density approximation turns out to be quite inadequate at low ionic strength.

Finally, two points are particularly noteworthy. First, the adopted model allows a simultaneous fit of nine SAS curves with only two free parameters, independent of the ionic strength, i.e., the non-electrostatic dissociation free energy and the monomer charge. This finding means that our simple interaction model is already able to describe the main structural features of the examined βLG solutions. Satisfactory results obtained by many other structural studies on colloidal or protein solutions, based upon similar very simplified models (Wagner et al., 1991; Krause et al., 1991; D'Aguanno and Klein, 1992; D'Aguanno et al., 1992; Nägele et al., 1993; Wanderlingh et al., 1994), suggest that the use of very refined potentials containing a large number of different contributions is often unnecessary, at least at the first stages of a research. Using sophisticated interaction models may even be nonsense when coupled with simultaneously rough treatment of the correlation functions, as is often the case with the widely used zeroth-order approximation, despite the fact that the introduction of a larger number of parameters can clearly improve the actual fitting of the data. Moreover, we have pointed out that, even in models with purely repulsive interactions, attractive effects (due to "osmotic depletion") are predicted by every sufficiently accurate theory. On the contrary, within the zero-density approximation for the RDFs, the same attractive effects may be reproduced only at the cost of adding artificial contributions to the potentials.

Second, the proposed first-order approximation to the RDFs is really able to yield accurate predictions for the average structure factor of weakly concentrated protein solutions, in a rather simple but physically sound way. It is worth stressing that the underlying calculation scheme is not restricted to the particular model considered in this paper, but may be easily applied to different spherically symmetric potentials. Although the limit of validity of the first-order approximation is still an open question, which we are planning to investigate in future work, we think that it may represent a new useful tool for the analysis of experimental SAS data of globular protein solutions, when their concentration is not too high and the strength of their interaction forces is not too large. When these two conditions fail, then it is unavoidable to compute the correlation functions by exploiting some more powerful method from the statistical mechanical theory of liquids (Hansen and McDonald, 1986). We hope, however, that this paper will stimulate the application of the proposed first-order approximation to different sets of experimental data on proteins, as well as new theoretical work on the quality and limit of this calculation scheme.

APPENDIX A

Calculation of protein form factors

In detail, the scattering particle is assumed to be homogeneous and its size and shape are described by the function $s(\mathbf{r})$, which gives the probability that the point $\mathbf{r} \equiv (r, \omega_r)$ (where ω_r indicates the polar angles α_r and β_r) lies within the particle. For compact particles, like globular proteins, this function can be written in terms of a unique two-dimensional angular shape function $\mathcal{F}(\omega_r)$, as

$$s(\mathbf{r}) = \begin{cases} 1 & r \leq \mathcal{F}(\omega_r) \\ \exp\{-[r - \mathcal{F}(\omega_r)]^2/2\sigma^2\} & r > \mathcal{F}(\omega_r) \end{cases} \quad \text{(A1)}$$

where σ is the width of the Gaussian that accounts for the particle hydration shell (Svergun et al., 1998). The shape function $\mathcal{F}(\omega_r)$ is evaluated by fixing the axis origin on the mean value of the atomic coordinates and running over each atom m and taking the maximum distance r between the origin and the intersection, if any, of the van der Waals sphere centered in m with the direction ω_r. Assuming homogeneous particles belonging to species i, M_i random points are generated from polar coordinates. The sampling is made for the variables α_r, $\cos \beta_r$, and r^3 in the ranges $[0, 2\pi]$, $[-1, 1]$ and $[0, r_{max}^3]$, respectively. Following Eq. A1, if $r \leq \mathcal{F}(\omega_r)$, the point is accepted, otherwise the probability $\mathcal{P} = \exp\{-[r - \mathcal{F}(\omega_r)]^2/2\sigma^2\}$ is calculated. A random number y between 0 and 1 is extracted and if $y < \mathcal{P}$ the point is accepted, otherwise it is rejected. The $p_i^{(1)}(r)$ histogram is then determined by taking into account the distances between the M_i points and the center, while the $p_i^{(2)}(r)$ histogram depends on the distances between all possible pairs of M_i points,

$$p_i^{(1)}(r) = \frac{1}{\Delta r M_i} \sum_{n=1}^{M_i} H(\Delta r/2 - |r - r_n|), \quad \text{(A2)}$$

$$p_i^{(2)}(r) = \frac{2}{\Delta r M_i(M_i - 1)} \sum_{n=1}^{M_i-1} \sum_{m=n+1}^{M_i} H(\Delta r/2 - |r - r_{nm}|),$$

$$\text{(A3)}$$

where Δr is the grid amplitude in the space of radial distance, r_n the distance between the center and the nth point. Here r_{nm} is the distance between the points n and m, and $H(x)$ is the Heaviside step function

$(H(x) = 0$ if $x < 0$ and $H(x) = 1$ if $x \geq 0$). The number of random scattering centers was $M_i = 2000$, the grid size was $\Delta r = 1$ Å, while the width of the surface mobility was fixed to $\sigma = 2$ Å.

APPENDIX B

First-order perturbative corrections

In the density expansion of the potentials of mean force $W_{ij}(r)$

$$-\beta W_{ij}(r) = -\beta u_{ij}(r) + \omega_{ij}^{(1)}(r)n + \omega_{ij}^{(2)}(r)n^2 + \ldots, \quad \text{(B1)}$$

the *exact* power coefficients $\omega_{ij}^{(k)}(r)$ $(k = 1, 2, \ldots)$ can be computed by using standard diagrammatic techniques (Meeron, 1958), which yield the results in terms of appropriate multidimensional integrals of products of Mayer functions

$$f_{ij}(r) = \exp[-\beta u_{ij}(r)] - 1 \quad \text{(B2)}$$

Within our approximation, we are only required to compute the first term, which involves a convolution and turns out to be

$$\omega_{ij}^{(1)}(r) = \sum_k x_k \gamma_{ij,k}^{(1)}(r)$$

$$= \sum_k x_k \int d\mathbf{r}' f_{ik}(r') f_{kj}(|\mathbf{r} - \mathbf{r}'|), \quad \text{(B3)}$$

where $x_k = n_k/n$ is the molar fraction of species k. The evaluation of the convolution integral $\gamma_{ij,k}^{(1)}(r)$ is not a difficult task in bipolar coordinates. Integration over angles is easily performed and $\gamma_{ij,k}^{(1)}(r)$ reduces to a double integral, which can be written as

$$\gamma_{ij,k}^{(1)}(r) = \frac{2\pi}{r} \int_0^\infty dx[x f_{ik}(x)] \int_{|x-r|}^{x+r} dy[y f_{kj}(y)]. \quad \text{(B4)}$$

We have evaluated all these $\gamma_{ij,k}^{(1)}(r)$ terms at the points $r_i = i\Delta r$ $(i = 1, \ldots, 500)$, with $\Delta r = 1$ Å. At each r_i value, the double integral has been carried out numerically, simply by using the trapezoidal rule for both x- and y-integration. For the x-integration, we have chosen as upper limit the value $x_{max} = \max(x_{cut}, R_2 + r)$, with $x_{cut} = R_2 + 12/\kappa_D$ (depending on the ionic strength), and as grid size $\Delta x = x_{cut}/200$. For the y-integration, $\Delta y = \Delta x$.

REFERENCES

Abis, S., R. Caciuffo, F. Carsughi, R. Coppola, M. Magnani, F. Rustichelli, and M. Stefanon. 1990. Late stages of δ' precipitation in an Al-Li alloy by small angle neutron scattering. *Phys. Rev. B.* 42:2275–2281.

Asakura, S., and F. Oosawa. 1954. On the interaction between two bodies immersed in a solution of macromolecules. *J. Chem. Phys.* 22:1255–1256.

Ashcroft, N. W., and D. C. Langreth. 1967. Structure of binary liquid mixtures. *Phys. Rev.* 156:685–692.

Baldini, G., S. Beretta, G. Chirico, H. Franz, E. Maccioni, P. Mariani, and F. Spinozzi. 1999. Salt induced association of β-lactoglobulin studied by salt light and x-ray scattering. *Macromolecules.* 32:6128–6138.

Blum, L., and J. S. Hoye. 1978. Solution of the Ornstein-Zernike equation with Yukawa closure for a mixture. *J. Stat. Phys.* 19:317–324.

Chacón, P., F. Morán, J. F. Díaz, E. Pantos, and J. M. Andreu. 1998. Low resolution structures of proteins in solution retrieved from x-ray scattering with a genetic algorithm. *Biophys. J.* 74:2760–2775.

Chen, S. H., and T. L. Lin. 1987. Collidal solutions. *In* Methods of Experimental Physics, Vol. 23: Neutron Scattering. D. L. Price and K. Sköld, editors. Academic Press, San Diego. 489–543.

D'Aguanno, B., and R. Klein. 1992. Integral equation theory of polydisperse Yukawa systems. *Phys. Rev. A.* 46:7652–7656.

D'Aguanno, B., R. Krause, J. M. Mendez-Alcaraz, and R. Klein. 1992. Structure factors of charged bidispersed colloidal suspensions. *J. Phys.: Condens. Matter.* 4:3077–3086.

Gasteiger, J., and M. Marsili. 1980. Iterative partial equalization of orbital electronegativity. A rapid access to atomic charges. *Tetrahedron.* 36:3219–3228.

Ginoza, M. 1990. Simple MSA solution and thermodynamic theory in a hard-sphere Yukawa system. *Mol. Phys.* 71:145–156.

Guinier, A., and G. Fournet. 1955. Small Angle Scattering of X-Ray. Wiley, New York.

Halgren, T. A., and W. Damm. 2001. Polarizable force fields. *Curr. Opin. Struct. Biol.* 11:236–242.

Hansen, J. P., and J. B. Hayter. 1982. A rescaled MSA structure factor for dilute charged colloidal dispersions. *Mol. Phys.* 46:651–656.

Hansen, J. P., and I. R. McDonald. 1986. The Theory of Simple Liquids. Academic Press, London.

Hayter, J. B., and J. Penfold. 1981. An analytic structure factor for macroion solutions. *Mol. Phys.* 42:109–118.

Henderson, S. J. 1996. Monte Carlo modeling of small-angle scattering data from noninteracting homogeneous and heterogeneous particles in solution. *Biophys. J.* 70:1618–1627.

Israelachvili, J. 1992. Intermolecular and Surface Forces, 2nd Ed. Academic Press, London.

Itri, R., and L. Amaral. 1991. Distance distribution function of sodium dodecyl sulfate micelles by x-ray scattering. *J. Phys. Chem.* 95:423–427.

Jacrot, B. 1976. The study of biological structures by neutron scattering from solution. *Rep. Prog. Phys.* 39:911–953.

Jacrot, B., and G. Zaccai. 1981. Determination of molecular weight by neutron scattering. *Biopolymers.* 20:2413–2426.

Kozin, M. B., V. V. Volkov, and D. I. Svergun. 1997. ASSA, a program for three-dimensional rendering in solution scattering from biopolymers. *J. Appl. Crystallogr.* 30:811–815.

Krause, R., B. D'Aguanno, J. M. Mendez-Alcaraz, G. Nägele, R. Klein, and R. Weber. 1991. Static structure factors of binary suspensions of charged polystyrene spheres: experiment against theory and computer simulation. *J. Phys.: Condens. Matter* 3:4459–4475.

Kuehner, D. E., C. Heyer, C. Rämsch, U. M. Fornefeld, H. W. Blanch, and J. M. Prausnitz. 1997. Interactions of lysozyme in concentrated electrolyte solutions from dynamic-light-scattering measurements. *Biophys. J.* 73:3211–3224.

Mariani, P., F. Carsughi, F. Spinozzi, S. Romanzetti, G. Meier, R. Casadio, and C. M. Bergamini. 2000. Ligand-induced conformational changes in tissue transglutaminase: Monte Carlo analysis of small-angle scattering data. *Biophys. J.* 78:3240–3251.

Meeron, E. 1958. Theory of potentials of average force and radial distribution functions in ionic solutions. *J. Chem. Phys.* 28:630–643.

Nägele, G. 1996. On the dynamics and structure of charge-stabilized suspensions. *Phys. Reports.* 272:215–372.

Nägele, G., T. Zwick, R. Krause, and R. Klein. 1993. Brownian motion in polydisperse charged colloidal suspensions. *J. Colloid Interface Sci.* 161:347–360.

Oliveira, K. M. G., V. L. Valente-Mesquita, M. M. Botelho, L. Sawyer, S. T. Ferreira, and I. Polikarpov. 2001. Crystal structures of bovine β-lactoglobulin in the orthorhombic space group C222$_1$. Structural differences between genetic variants A and B and features of the Tanford transition. *Eur. J. Biochem.* 268:477–484.

Parsegian, V. A., and E. A. Evans. 1996. Long and short range intermolecular and intercolloidal forces. *Curr. Opin. Struct. Biol.* 1:53–60.

Rogers, F. J., and D. A. Young. 1984. New, thermodynamically consistent, integral equation for simple fluids. *Phys. Rev. A.* 30:999–1007.

Ruiz-Estrada, H., M. Medina-Noyola, and G. Nägele. 1990. Rescaled mean spherical approximation for colloidal mixtures. *Physica A.* 168:919–941.

Sheinerman, F. B., R. Norel, and B. Honig. 2000. Electrostatic aspects of protein-protein interactions. *Curr. Opin. Struct. Biol.* 10:153–159.

Spinozzi, F., F. Carsughi, and P. Mariani. 1998. Particle shape reconstruction by small-angle scattering. Integration of group theory and maximum entropy to multipole expansion method. *J. Chem. Phys.* 109:10148–10158.

Svergun, D. I., C. Barberato, and M. H. J. Koch. 1995. CRYSOL: a program to evaluate x-ray solution scattering of biological macromolecules from atomic coordinates. *J. Appl. Crystallogr.* 28:768–773.

Svergun, I., S. Richard, M. H. J. Koch, Z. Sayers, S. Kuprin, and G. Zaccai. 1998. Protein hydration in solution: experimental observation by x-ray and neutron scattering. *Proc. Natl. Acad. Sci. USA.* 95:2267–2272.

Svergun, D. I., V. V. Volkov, M. B. Kozin, H. B. Stuhrmann, C. Barberato, and M. H. J. Koch. 1997. Shape determination from solution scattering of biopolymers. *J. Appl. Crystallogr.* 30:798–802.

Velev, O. D., E. W. Kaler, and A. M. Lenhoff. 1997. Protein interactions in solution characterized by light and neutron scattering: comparison of lysozyme and chymotrypsinogen. *Biophys. J.* 75:2682–2697.

Vervey, E. J., and J. Th. G. Overbeek. 1948. Theory of the Stability of Lyophobic Colloids. Elsevier, Amsterdam.

Wagner, N. J., R. Krause, A. R. Rennie, B. D'Aguanno, and J. Goodwin. 1991. The microstructure of polydisperse, charged colloidal suspensions by light and neutron scattering. *J. Chem. Phys.* 95:494–508.

Wanderlingh, U., R. Giordano, and G. Giunta. 1994. Structure in protein solution changing the pH. *Il Nuovo Cimento.* 16:1493–1498.

Zerah, G., and J. P. Hansen. 1986. Self-consistent integral equations for fluid pair distribution functions: another attempt. *J. Chem. Phys.* 84:2336–2343.